Transition from mass asymmetry to symmetry in the spontaneous fission of Fm isotopes*

M. G. Mustafa
Department of Physics and Astronomy, University of Maryland, College Park, Maryland 20742
(Received 5 August 1974)

The observed transition in the spontaneous fission mass distribution from asymmetry in the lighter Fm isotopes to symmetry in the heavier Fm isotopes is studied on the basis of the potential energy surfaces (PES) and fragment shell effects in the two-center shell model. To that end, we have calculated the PES for ^{256}Fm and compared them with our previous PES results for other Fm isotopes. Our calculations show that the lighter Fm isotopes (up to ^{256}Fm) should fission asymmetrically, while ^{258}Fm and other heavier Fm isotopes should fission symmetrically. This is due to the fact that the shell corrections in these nuclei are found to increase with increasing mass number and decreasing neck radius, particularly in the region beyond the second barrier. This, in turn, is a consequence of strong shell effects in fragment nuclei near the doubly closed-shell $^{132}_{50}Sn_{82}$. The results supporting these conclusions are shown.

[NUCLEAR STRUCTURE Spontaneous fission ^{252,256,258,264}Fm; calculated shell corrections and potential energy surfaces; asymmetric two-center shell model; transition from mass asymmetry to symmetry.]

Recent experiments on spontaneous[1-4] and low-energy neutron induced fission[1,5] of Fm isotopes have shown that a transition in the mass distribution from asymmetry to symmetry occurs between ^{256}Fm and ^{258}Fm. This trend towards mass symmetry has been reviewed by Hoffman.[6]

In our previous work,[7] we have indicated that the transition in the mass distribution of Fm isotopes is a consequence of fragment shell effects. In this paper, we propose to extend that idea and show in detail the role of fragment shell effects in the spontaneous fission of Fm isotopes. To that end, we have found it necessary to calculate the potential energy surfaces (PES) for ^{256}Fm in the two-center shell model and compare them with our previous PES calculations for ^{252}Fm, ^{258}Fm, and ^{264}Fm.[7]

We will therefore briefly outline the model used in the PES calculation. After that, we present our PES results for ^{256}Fm and compare them with other Fm isotopes. The fragment shell effects are then shown as a function of the mass number of Fm isotopes and also as a function of the neck parameter D (see below) to explain the transition from mass asymmetry to symmetry.

The potential energy of a deformed nuclear shape is obtained from the sum of the liquid drop model (LDM) energy[8] and the Strutinsky shell correction energy with pairing.[9] The LDM energy is calculated by Myers-Swiatecki mass formula[8] and the shell corrections are calculated by the two-center shell model for asymmetric shapes.[7,10]

Since the single particle model used in the present work is the same as that used in our earlier calculations for asymmetric fission, we shall omit the mathematical details here. However, the quantities necessary for the presentation of results are defined.

In this model, we need four independent shape parameters to describe the nuclear shape: D, the neck radius in fm; λ, the volume (mass) ratio of the portions of the nucleus on either side of the neck plane ($\lambda = 1$ for symmetry); $\alpha = a_2/a_1 - 1$; and $\sigma = z_1/[\sqrt{2}c_1] = z_2/[\sqrt{2}c_2]$. Here a_1 and a_2 are the ρ semiaxes and c_1 and c_2 are z semiaxes of the two half spheroids connected by a smooth neck. z_1 and z_2 are the centers of the half spheroids (see Fig. 1 in Ref. 7).

The strength parameters associated with the spin-orbit and $\vec{l}^2$ term of the deformed single particle potential and the pairing strengths for the BCS calculations are the same as those used in Ref. 7.

We now present the results of the potential energy surface calculations for ^{256}Fm and compare them with other Fm isotopes. The fragment shell effects are then shown as a function of the mass number of Fm isotopes and also as a function of the constriction degree of freedom, i.e., the neck radius D.

Since the calculations of the full four-dimensional (D, λ, α, σ) potential energy surfaces (PES) are very time consuming, our calculations are restricted to cuts $V(\lambda)$ (i.e., the potential energy as a function of λ, the volume ratio) for selected values of the neck radius D around and beyond the second saddle point. We shall see later that it is sufficient to compare $V(\lambda)$ cuts for various Fm isotopes to explain quantitatively the transition from mass asymmetry to symmetry. We should

note that the potential energies are minimized with respect to α and σ.

Figure 1 shows the potential energy for ^{256}Fm as a function of λ, the volume ratio, for selected values of the neck radius D. The energies are normalized to the ground state of the nucleus and as has been mentioned earlier, the energies are minimized with respect to α and σ. The elimination of α and σ by minimization is not meant to imply that the fissioning system always follows the minimum energy path; rather, this procedure just permits the display of results in terms of two most important fission variables λ and D.

D = 5.0 fm is the region around the second barrier and the smaller values of D indicate the minimum energy path towards scission. The figure shows that the fissioning nucleus ^{256}Fm prefers symmetry around the second barrier and then slowly becomes asymmetric with decreasing D. We should note that the difference in the energy between symmetry and asymmetry is very small

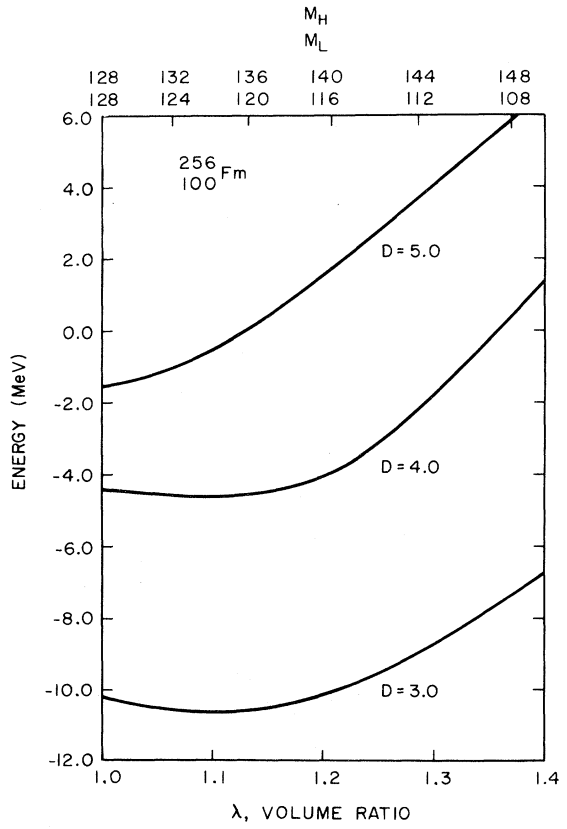

FIG. 1. The potential energy for ^{256}Fm as a function of λ, the volume ratio of the portions of the nucleus on either side of the neck plane, for selected values of D, the radius of the neck in fermis. The energy has been minimized with respect to α and σ and normalized to zero for the ground state energy.

(for D = 3.0 fm, it is about 0.5 MeV). The extension of the calculation to smaller D is not expected to significantly increase the energetic preference for asymmetry (see Ref. 7 for our calculations on ^{252}Fm and ^{258}Fm).

Thus our PES calculation indicates a small energetic preference for mass asymmetry for the spontaneous fission of ^{256}Fm. Based on their analysis of the fission probabilities over the outer barrier, Tsang and Wilhelmy[11] also arrived at the same conclusion for the spontaneous fission of this nucleus. However, their prediction of asymmetric spontaneous fission for ^{258}Fm disagrees with our calculation (Ref. 7); we have found a preference for symmetric fission.

In Fig. 2(a), we have compared the potential energies for ^{252}Fm, ^{256}Fm, ^{258}Fm, and ^{264}Fm, as a function of volume ratio λ for shapes near the second saddle point. The energies are normalized to the ground state of respective nuclei. We should note that there is no second saddle for ^{258}Fm and ^{264}Fm. However, for the purpose of comparison, we have chosen D = 5.0 fm which corresponds to the second saddle point in ^{256}Fm. The figure shows that in the second saddle region the preferred shapes are reflection symmetric. However, with decreasing neck radius D, we find that the preference changes from symmetry to asymmetry in ^{252}Fm and ^{256}Fm, while the preferred shapes in ^{258}Fm and ^{264}Fm are still reflection symmetric. This is shown in Fig. 2(b), where $V(\lambda)$ is plotted for D = 4.0 fm. Figure 2(b) is a clear demonstration of the fact that the lighter Fm isotopes prefer asymmetric mass division, while the heavier Fm isotopes prefer symmetric mass division. The transition from asymmetry to symmetry occurs in the Fm mass region $256 < A < 258$ (also see Fig. 3).

For smaller values of D, a similar result can be found and for a comparison, we refer to Fig. 1 in this paper and to Figs. 9–11 of Ref. 7.

Figure 3 is a special case of Fig. 2, where the potential energy is plotted as a function of the mass number of Fm isotopes for the symmetric shapes (solid line) and the asymmetric shapes (dashed line). The asymmetric shapes are λ = 1.1 for ^{256}Fm, ^{258}Fm, and ^{264}Fm and λ = 1.25 for ^{252}Fm [see Fig. 2(b)]. The choice of λ = 1.1 for ^{258}Fm and ^{264}Fm is arbitrary, while λ = 1.1 for ^{256}Fm and λ = 1.25 for ^{252}Fm represent the minimum potential energy shapes for the neck radius D = 4.0 fm. A straight line is drawn between calculated points. The figure provides a simpler demonstration of the transition from mass asymmetry to symmetry in the Fm isotopes and is also used as a reference for Figs. 4 and 5.

In order to examine the role of fragment shell

effects in this transition from asymmetric mass division to symmetric mass division in Fm isotopes, we have plotted in Fig. 4 the shell correction energies as a function of the mass number of Fm isotopes for both the symmetric and the shell correction energy preferred asymmetric shapes. The asymmetry in ^{252}Fm is $\lambda = 1.25$, in ^{256}Fm $\lambda = 1.1$, and in ^{258}Fm $\lambda = 1.1$, and for all the shapes the neck radius is kept fixed at $D = 4.0$ fm. Figure 4 shows two important results:

(a) The shell corrections prefer asymmetric shapes for $A < 264$ and this preference increases with decreasing mass number of Fm isotopes. Similar results are also found for other values of D between the second barrier and the scission point. The shell preference of symmetry for the constricted shapes in ^{264}Fm is due to the fact that two double-magic $^{132}_{50}Sn_{82}$ fragments are formed at symmetry. For further discussion on this we refer to Refs. 7 and 12. The LDM, however, always prefer symmetric shapes. The competition between the two energies, i.e., the shell correction energies and the LDM energies, finally decides the mass number where the asymmetric mass division should become symmetric (see Fig. 3).

(b) Figure 4 also shows how the shell corrections are increasing with the mass number of Fm isotopes, for both symmetric and asymmetric shapes. This is a direct consequence of strong shell effects in fragment nuclei near doubly closed-shell $^{132}_{50}Sn_{82}$.

The plots similar to Figs. 3 and 4 for second saddle shapes of Fig. 2(a) are not meaningful in the present context, since all the Fm isotopes show a preference for reflection symmetry.

The shell corrections are also found to increase in magnitude with constriction, i.e., decreasing D. A typical example is shown in Fig. 5, where the shell corrections for the minimum potential energy shapes of ^{258}Fm are plotted as a function of neck radius, D. (We note that the minimum energy shapes for this nucleus are symmetric, $\lambda = 1$.)

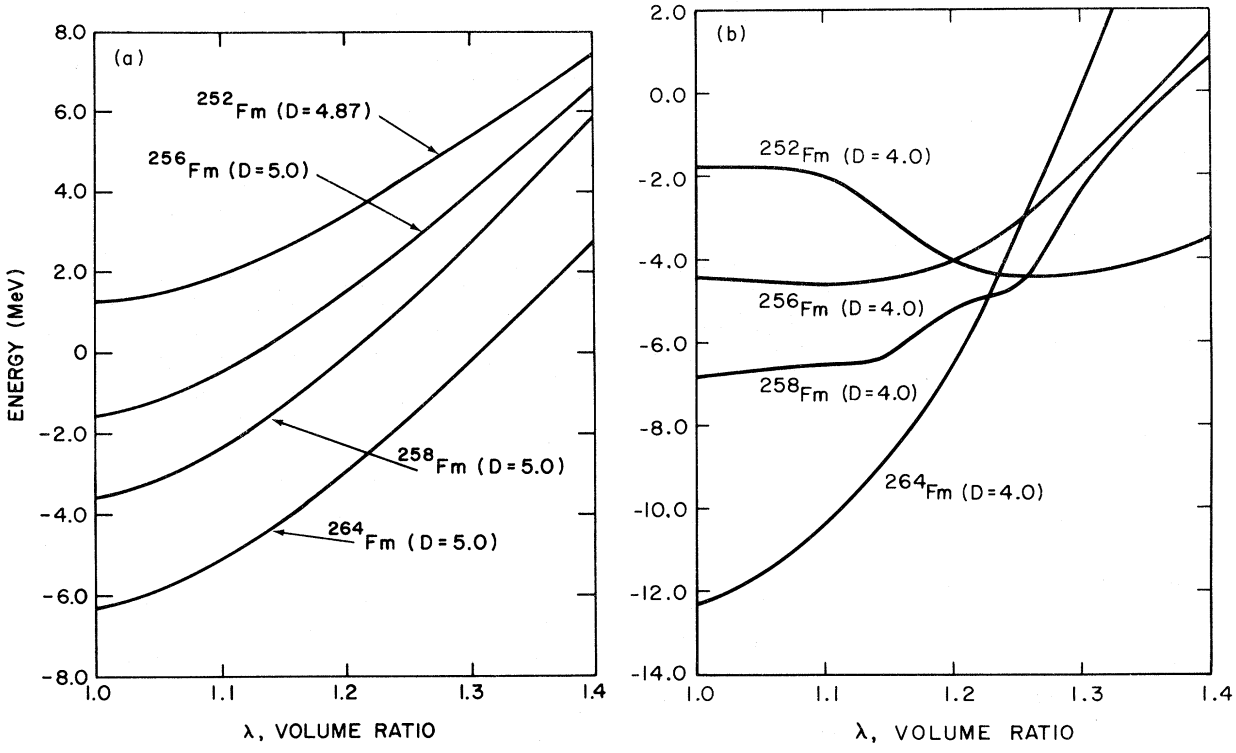

FIG. 2. (a) The potential energies for ^{252}Fm, ^{256}Fm, ^{258}Fm, and ^{264}Fm are plotted as a function of λ, the volume ratio of the portions of the nucleus on either side of the neck plane, for the shapes near the second saddle point. The energies have been minimized with respect to α and σ and normalized to zero for the ground state energy of respective nuclei. The results for ^{252}Fm, ^{258}Fm, and ^{264}Fm are taken from Ref. 7. (b) The potential energies for ^{252}Fm, ^{256}Fm, ^{258}Fm, and ^{264}Fm are plotted as a function of λ, the volume ratio of the portions of the nucleus on either side of the neck plane, for the fixed value of the neck radius $D = 4.0$ fm. The energies have been minimized with respect to α and σ and normalized to zero for the ground state energy of respective nuclei. The results for ^{252}Fm, ^{258}Fm, and ^{264}Fm are taken from Ref. 7.

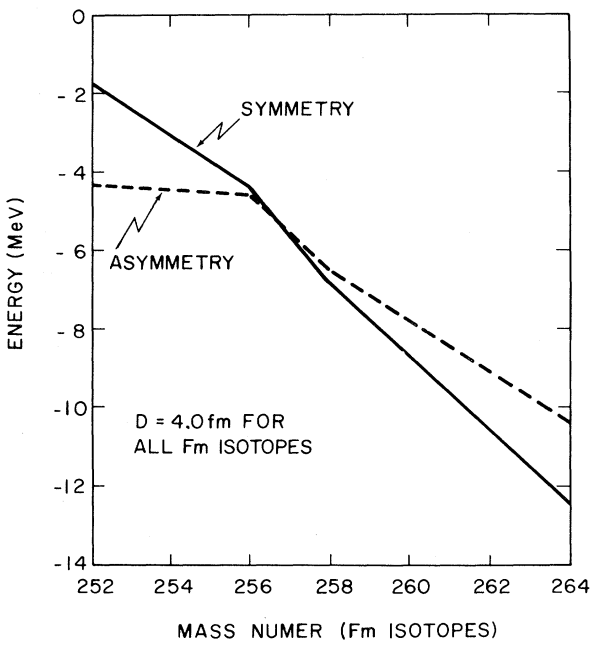

FIG. 3. The potential energy is plotted as a function of the mass number of Fm isotopes for symmetric (solid line) and asymmetric (dashed line) shapes. The energies are taken from Fig. 2(b). The asymmetric shapes are $\lambda = 1.1$ for ^{256}Fm, ^{258}Fm, and ^{264}Fm and $\lambda = 1.25$ for ^{252}Fm. A straight line is drawn between calculated points.

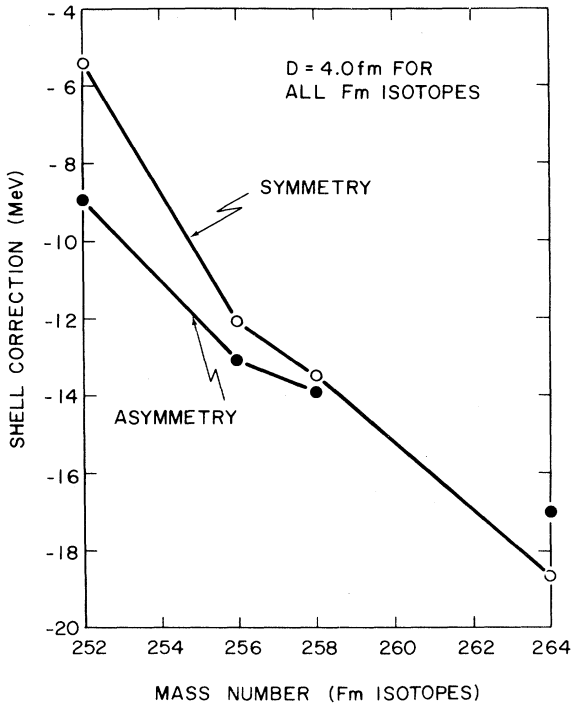

FIG. 4. The shell correction energies are shown as a function of the mass number of Fm isotopes for symmetric ($\lambda = 1$) and shell energy preferred asymmetric shapes. The asymmetric shapes are $\lambda = 1.1$ for ^{258}Fm, $\lambda = 1.1$ for ^{256}Fm, and $\lambda = 1.25$ for ^{252}Fm. A straight line is drawn between calculated points. Also shown is the shell correction energy for $\lambda = 1.1$ in ^{264}Fm.

This shows that the nascent fragment structure effect increases in the descent from the second barrier to the scission point.

We have thus shown that the shell corrections in Fm isotopes increase with increasing mass number and with decreasing neck radius D in the region between the second barrier and the scission point. As a result, the transition from mass asymmetry to symmetry is seen to occur not at the second saddle point but beyond it. For a statistical model interpretation of this transition, we refer to Ref. 13.

The potential energy surfaces for ^{256}Fm have been calculated with the two-center shell model. The results indicate a small energetic preference for asymmetric mass division in this nucleus.

The potential energy surfaces for ^{252,256,258,264}Fm are compared for shapes near the second saddle point and also for shapes with the neck radius $D = 4.0$ fm (beyond the second saddle point). We have seen that a transition from fission fragment mass asymmetry to symmetry should occur between ^{256}Fm and ^{258}Fm. This is shown to be a consequence of the fact that the fragment shell effects increase with increasing mass number of Fm isotopes. For the shapes with $D = 4.0$ fm, we have ex-

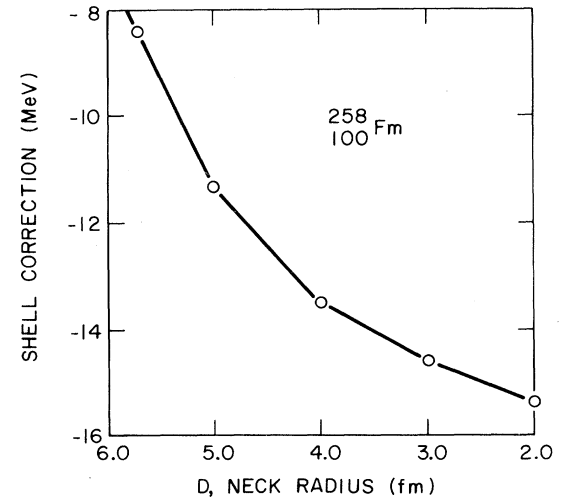

FIG. 5. The shell correction energies for the minimum potential energy shapes of ^{258}Fm are shown as a function of D, the radius of the neck in fermis. The minimum potential energy shapes are found to be symmetric ($\lambda = 1$) (Ref. 7). A straight line is drawn between calculated points.

plicitly shown the shell corrections for the Fm isotopes studied in this paper (Fig. 4). We have also shown that the fragment shell effects increase with decreasing neck radius D (Fig. 5). As a result, the transition from asymmetry to symmetry is seen to occur not at the second saddle point but just beyond it.

The author wishes to acknowledge helpful discussions with C. Y. Wong and J. J. Griffin.

---

*Work supported by the U. S. Atomic Energy Commission.

[1]W. John, E. K. Hulet, R. W. Lougheed, and J. J. Wesolowski, Phys. Rev. Lett. 27, 45 (1971).

[2]J. P. Balagna, G. P. Ford, D. C. Hoffman, and J. D. Knight, Phys. Rev. Lett. 26, 145 (1971).

[3]K. F. Flynn, E. P. Horwitz, C. A. A. Bloomquist, R. F. Barnes, R. K. Sjoblom, P. R. Fields, and L. E. Glendenin, Phys. Rev. C 5, 1725 (1972).

[4]R. M. Harbour, K. W. MacMurdo, D. E. Troutner, and M. V. Hoehn, Phys. Rev. C 8, 1488 (1973).

[5]R. C. Ragaini, E. K. Hulet, R. W. Lougheed, and J. Wild, Phys. Rev. C 9, 399 (1974).

[6]D. C. Hoffman, Los Alamos Report No. LA-DC-72-898, August, 1972 (unpublished).

[7]M. G. Mustafa, U. Mosel, and H. W. Schmitt, Phys. Rev. C 7, 1519 (1973). A preliminary report appeared in Phys. Rev. Lett. 28, 1536 (1972).

[8]W. D. Myers and W. J. Swiatecki, Ark. Fys. 36, 343 (1967). However, the surface symmetry coefficient has been changed from 1.7826 to 2.53. For a discussion on this, we refer to Ref. 7.

[9]V. M. Strutinsky, Nucl. Phys. A122, 1 (1968).

[10]U. Mosel, J. Maruhn, and W. Greiner, Phys. Lett. 35B, 125 (1971).

[11]C. F. Tsang and J. B. Wilhelmy, Nucl. Phys. A184, 417 (1972).

[12]H. W. Schmitt and U. Mosel, Nucl. Phys. A186, 1 (1972).

[13]P. Fong, Phys. Rev. C 9, 2448 (1974).